PRAMANA
— journal of
physics

Vol. 85, No. 6
December 2015
pp. 1245–1255

The effect of surface plasmon resonance on optical response in dielectric (core)–metal (shell) nanoparticles

S FARJAMI SHAYESTEH* and MATIN SAIE

Department of Physics, University of Guilan, Rasht, Guilan 4193833697, Iran
*Corresponding author. E-mail: saber@guilan.ac.ir

MS received 22 May 2013; revised 6 August 2014; accepted 26 September 2014
DOI: 10.1007/s12043-015-0950-7; ***e*Publication:** 18 June 2015

Abstract. In this work, we present the effect of refractive index of an embedding medium, core and shell having various sizes of metallic nanoshells on the surface plasmon resonance (SPR) properties in the spherical dielectric–metal core–shell nanoparticles based on the quasistatic approaches and Mie theory. For the metallic nanoshell with dimensions comparable to the wavelength of light, the quasistatic approximation shows good agreement with the Mie theory results. However, for large nanoparticles the quasistatic approximation is not appropriate and Mie theory illustrates SPR due to dipole and quadrupole in extinction cross-section. The typical cross-section calculations show two peaks that related to inner and outer surfaces. The dimensional dependence of optical constant in the Drude model leads to a decrease in plasma absorption in metal core–shell. By increasing the shell radius and therefore increasing the metal content the SPR at the outer surface shifts to higher energy and the weaker peak (at inner surface) shifts to lower energy. Also, depending on the metal shell materials SPR occurs in different energy regions and therefore can be tuned the SP frequency at higher energy by changing the shell materials. In addition, SPR frequency is sensitive to variation in refractive index of the environment of core-shell.

Keywords. Metal nanoshell; surface plasmon resonance; optical properties.

PACS Nos 78.67.Bf; 73.20.Jc; 78.40.Kc

1. Introduction

Metal nanoshells are dielectric (core)–metal (shell) nanoparticles that exhibit unique optical properties due to their interaction with the electromagnetic field which is greatly intensified by a phenomenon known as the surface plasmon resonance (SPR). This resonance effect arises from the collective oscillations of the conduction electrons in the metal shell, which efficiently couple to the incident electromagnetic field, and propagate along the surface [1–7]. At the plasmon resonance frequency the absorption cross-section of the nanoshell can be enhanced several times that is expected from the geometrical cross-section of the particle [8–11]. Also, plasmonic metallic nanoshell has received considerable attention because of its chemical sensing and biological analysing properties. It has

been recognized since 1951 that core–shell nanoparticles have versatile optical properties, despite the fact probably only they became more widely appreciated after a series of publications and patents by the group of Halas in the USA [12–14]. It was demonstrated that a thin shell of metal such as Au surrounding a spherical dielectric core exhibits two surface plasmon resonances associated with the outer and inner surfaces of the shell. As the shell thickness is decreased the two surface plasmons will interact with each other more strongly and hence shift in position relative to the position of the individual resonances of the sphere surface or cavity occurs [15,16]. For nanoshells with dimensions much smaller than the incident wavelength, the quasistatic approach is appropriate for calculating the influence of refractive index of the materials on SPR [17]. If the particles size is larger than the quasistatic limit, the Mie theory is applicable and higher multipole modes dominate in the calculated extinction cross-section spectra [18]. The time-dependent local density approximation (TDLDA) [19] and discrete dipole approximation (DDA) [20] are some methods for investigating the properties of metal nanoshell. Using these methods and with the development of computers, simulation of scattering and extinction coefficient data for comparison with the experimental data and prediction of optical properties is possible.

In this work, we explain the effects of refractive index of the shell, core and the embedded medium and various sizes of the nanoshell on the extinction cross-section based on the quasistatic approximation and Mie theory and later compare the results of these approaches. For bigger nanostructures the Mie theory is used to study the multipolar plasmon frequencies. Also, by using Mie theory the effect of surface plasmon on the optical properties of Au, Ag, Li, Na and Cs metal nanoshells were investigated. In this investigation, size and metallic content in the core–shell is crucial.

2. Theory

2.1 *Dielectric function*

Some of the metal properties, including optical properties can be described with the simple free-electron gas Drude–Sommerfeld model of dielectric function. In the framework of this model, by applying an external field, the conduction electrons move freely between independent collisions occurring at the average rate of the frequency-dependent dielectric function $\varepsilon(\omega)$ predicted by the Drude–Sommerfeld model:

$$\varepsilon(\omega) = \varepsilon_{\mathrm{b}} - \frac{\omega_{\mathrm{p}}^2}{\omega\,(\omega + i\gamma)}, \tag{1}$$

where ε_{b} is the phenomenological parameter describing the contribution of bound electrons to polarizability, ω_{p} is the bulk plasmon frequency

$$\omega_{\mathrm{p}}^2 = \frac{ne^2}{\varepsilon_0 m^*},$$

where n is the free electron concentration, m^* is the effective mass of the electron, e is the charge of the electron and γ is the phenomenological electron damping constant of the bulk material. For Au, $\varepsilon_{\mathrm{b}} = 9.8$ eV, $\gamma = 0.066$ eV and $\omega_{\mathrm{p}} = 9$ eV [21].

The dimensional dependence of the dielectric function was introduced within the framework of the model of limitation of the mean free path of conduction electrons [22]. Decreasing the size of a nanoparticle will eventually cause the thickness to become less than the bulk mean free path, and electron scattering from the surfaces of the particle will have decreasing effect thus broadening its plasmon resonance peaks. If the electron mean free path depends on size of the nanoparticles, a correction is available for the nanoshells and in this case, γ can be modified to [9]:

$$\gamma = \gamma_{\text{bulk}} + A\frac{v_{\text{F}}}{r_{\text{eff}}} \tag{2}$$

where γ_{bulk} is the damping constant of the bulk material, v_{F} is the electron velocity at the Fermi surface, A is an empirical parameter used for matching the calculated damping with the experimental result and r_{eff} is the effective mean free path of collisions and can be calculated from [23]

$$r_{\text{eff}} = \frac{\{(r_{\text{shell}} - r_{\text{core}})\,(r_{\text{shell}}^2 - r_{\text{core}}^2)\}^{1/3}}{2}, \tag{3}$$

where r_{shell} is the outer shell radius and r_{core} is the core (inner shell) radius. In calculations, it was assumed that the dielectric constant owing its origin to the contribution of bound electrons is independent of the geometric parameters of the particles.

2.2 *Quasistatic approximation (the dipole approximation)*

When the particle size is much smaller than the incident wavelength (for Au particle it is about 25 nm), the incident electric field may be regarded as being spatially uniform over the extent of the particle; so that the particle can be replaced by an oscillating dipole and this is referred to as the quasistatic approximation [9,24]. The advantage of this approximation is that the equations became simple considerably and spherical Bessel functions need not be calculated. Expressions for the electric field in the quasistatic approximation are obtained by letting the wavelength tend to infinity relative to the particle size. The scattering, extinction and absorption cross-sections are given as

$$\sigma_{\text{sca}}(\omega) = \frac{8\pi^2\omega^4}{3c^4}\,|\alpha(\omega)|^2\,, \tag{4}$$

$$\sigma_{\text{ext}}(\omega) = \frac{2\pi\omega}{c}\text{Im}(\alpha(\omega)), \tag{5}$$

$$\sigma_{\text{abs}}(\omega) = \sigma_{\text{ext}}(\omega) - \sigma_{\text{sca}}(\omega), \tag{6}$$

where c is the speed of light, ω is the angular frequency and α is the complex polarizability of the particle.

$$\alpha = 4\pi\, r_{\text{shell}}^2\, \frac{(\varepsilon_{\text{shell}} - \varepsilon_{\text{m}})\,(\varepsilon_{\text{core}} + 2\varepsilon_{\text{shell}}) + f\,(\varepsilon_{\text{core}} - \varepsilon_{\text{shell}})\,(\varepsilon_{\text{m}} + 2\varepsilon_{\text{shell}})}{(\varepsilon_{\text{shell}} + 2\varepsilon_{\text{m}})\,(\varepsilon_{\text{core}} + 2\varepsilon_{\text{shell}}) + f\,(2\varepsilon_{\text{shell}} - 2\varepsilon_{\text{m}})\,(\varepsilon_{\text{core}} - \varepsilon_{\text{shell}})}, \tag{7}$$

where $\varepsilon_{\text{core}}$, $\varepsilon_{\text{shell}}$ and ε_{m} are the dielectric functions of the core, shell and surrounding medium, respectively, and $f = (r_{\text{core}}/r_{\text{shell}})^{1/3}$ is the fraction of the total particle volume occupied by the core.

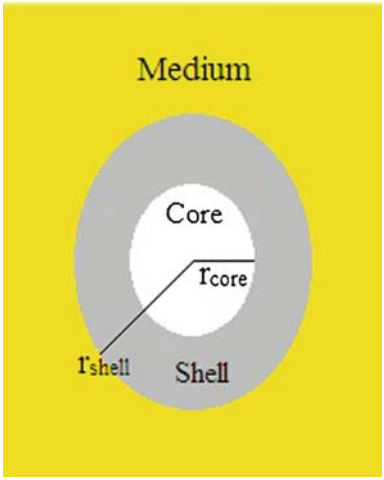

Figure 1. Schematic representation of the metal nanoshell with dielectric (core) and metal (nanoshell).

2.3 *Mie theory*

The Mie scattering theory [25–27] provides complete analytical solutions of Maxwell's equations for the scattering of electromagnetic radiation by particles with spherical or cylindrical symmetry. Aden and Kerker have published complete details of scattering from concentric spherical shells in 1951 [28]. In Mie theory, the harmonically oscillating electromagnetic fields are expressed in terms of a set of spherical vector basis functions such that each term in the expansion represents one of the resonances. Mie theory is a versatile technique for determining the optical properties of nanoshells or any other spherical particles of any dimension. The spherical symmetry suggests the use of a multipole extension of the fields, providing Mie's calculations a series of multipole oscillations (dipole, quadrupole etc.) for the absorption and scattering cross-section calculations of the particles as a function of particle radius. The extinction spectrum is a sum of absorption and scattering modes, each of which has a contribution depending on the particle size. Higher-order modes become more dominant with the increasing particle size. Physically, this can be explained by the fact that for larger particles, the light cannot polarize the

Table 1. Structural parameters [21,27] used in numerical calculation.

Material	e_∞	ω_p (eV)	γ_{bulk} (eV)	A
Au	9.80	9.0	0.066	0.25
Ag	3.70	8.9	0.018	0.25
Na	1.00	5.6	0.030	0.10
Li	5.84	8.0	0.050	0.10
Cs	1.00	3.4	0.020	0.10

nanoparticles homogeneously and retardation effects lead to the excitation of higher-order modes [9,26]. The Mie scattering, extinction and absorption efficiencies are given by

$$\sigma_{\text{ext}} = \frac{\lambda^2}{2\pi} \sum_{L=1}^{\infty} (2L+1)\text{Re}(a_L + b_L), \tag{8}$$

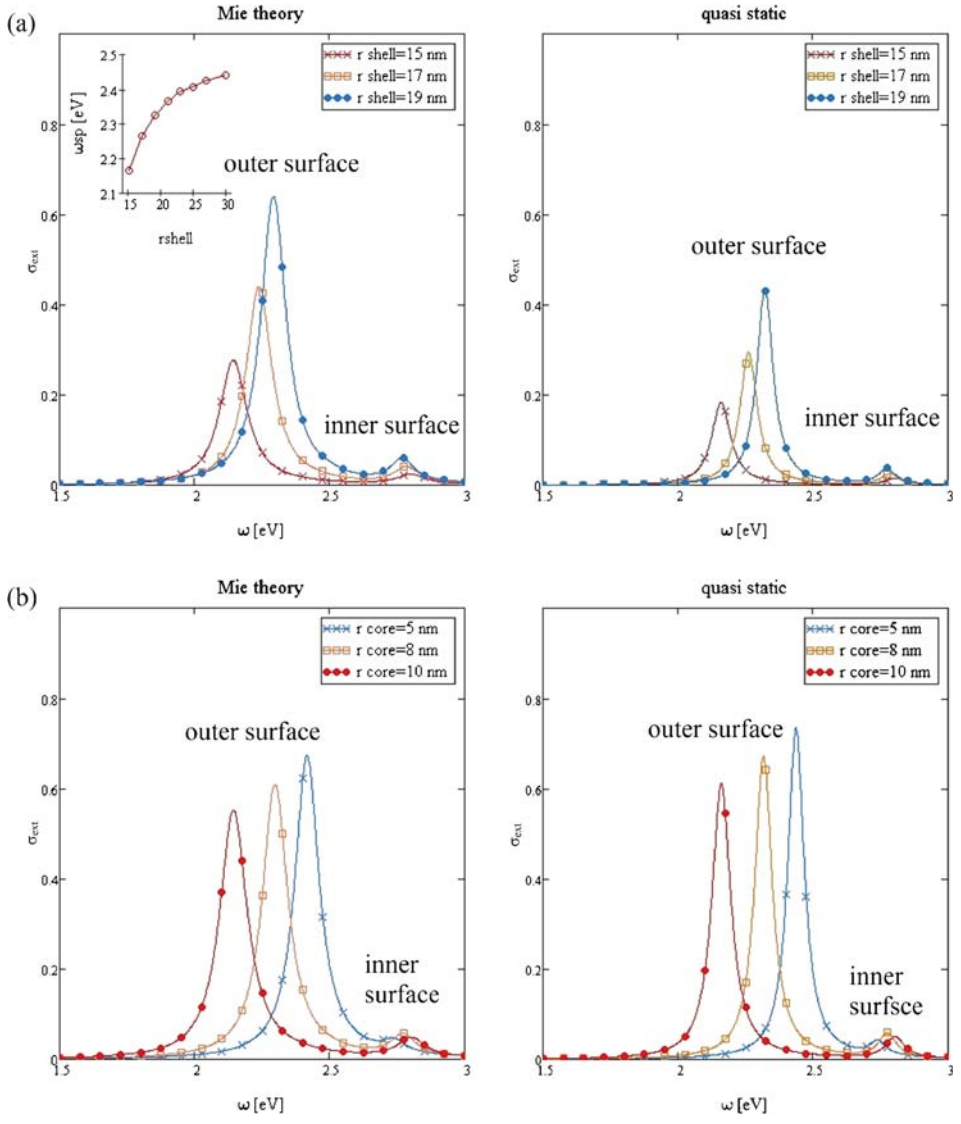

Figure 2. The extinction cross-section calculated for gold nanoshells using quasistatic approximation and Mie theory, (**a**) for core radius of 10 nm and different outer shell radii of 15, 17, 19 nm and (**b**) for a constant outer radius of 15 nm and different radii of the core embedded in a medium with $n_{\text{out}} = 1.5$. Inset shows the SPR response to a range of outer radii of the shell.

$$\sigma_{\text{scat}} = \frac{\lambda^2}{2\pi} \sum_{L=1}^{\infty} (2L+1)\left(|a_L|^2 + |b_L|^2\right), \tag{9}$$

$$\sigma_{\text{abs}} = \sigma_{\text{ext}} - \sigma_{\text{scat}}, \tag{10}$$

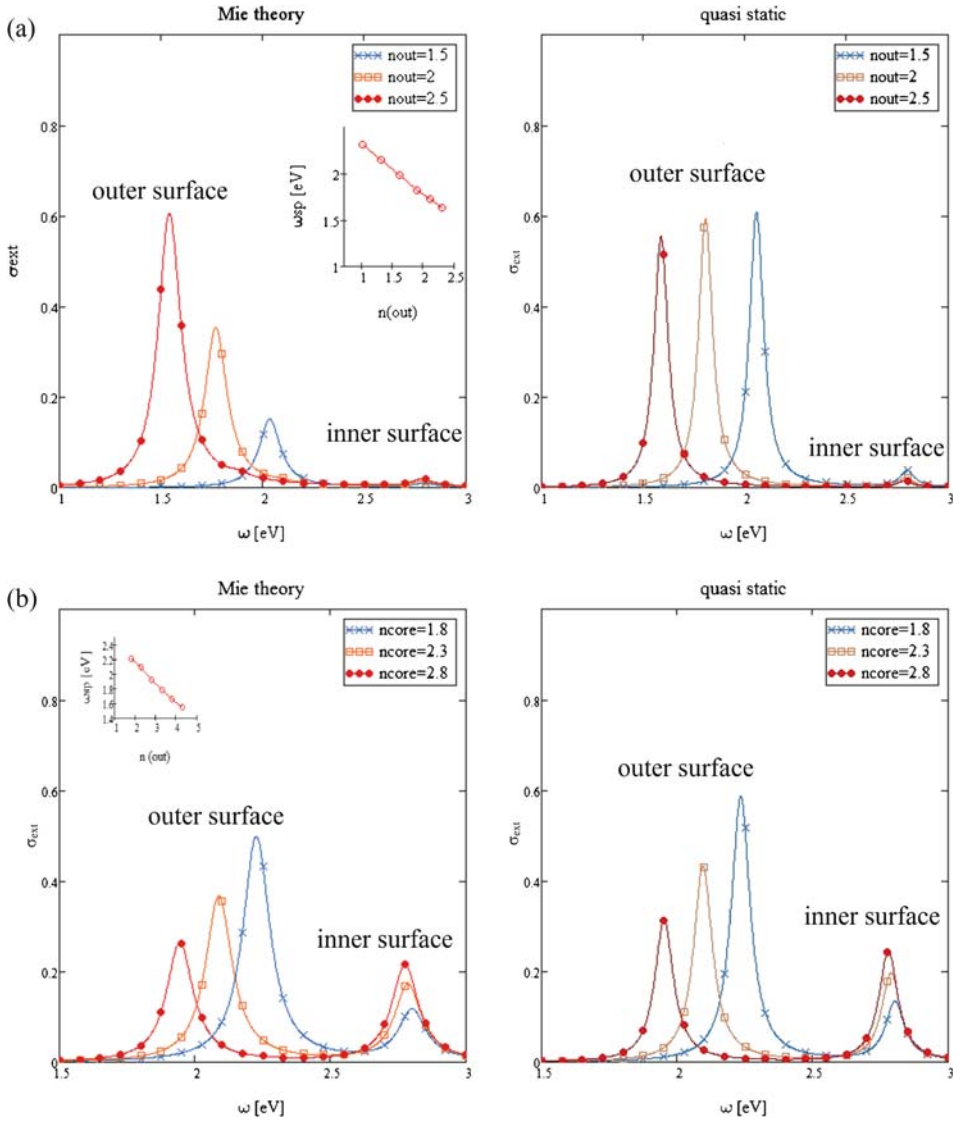

Figure 3. The extinction cross-section calculated for gold nanoshells using quasistatic approximation and Mie theory for (**a**) different embedding medium refractive index with $n_{\text{core}}(SiO_2) = 1.5$ and (**b**) the different core with $n_{\text{out}}(H_2O) = 1.3$. $r_{\text{core}} = 10$ nm and $r_{\text{shell}} = 15$ nm.

where a_L and b_L are the scattered field expansion coefficients and λ is the incident light wavelength.

$$a_L = \frac{\psi_L(y)\,(\psi'_L(m_2y) - A_L\chi'_L(m_2y)) - m_2\psi'_L(y)\,(\psi_L(m_2y) - A_L\chi_L(m_2y))}{\xi(y)\,(\psi'_L(m_2y) - A_L\chi'_L(m_2y)) - m_2\xi'_L(y)\,(\psi_L(m_2y) - A_L\chi_L(m_2y))}, \tag{11}$$

$$b_L = \frac{m_2\psi_L(y)\,(\psi'_L(m_2y) - B_L\chi'_L(m_2y)) - \psi'_L(y)(\psi_L(m_2y) - B_L\chi_L(m_2y))}{m_2\xi(y)\,(\psi'_L(m_2y) - B_L\chi'_L(m_2y)) - \xi'_L(y)(\psi_L(m_2y) - B_L\chi_L(m_2y))}, \tag{12}$$

$$A_L = \frac{m_2\psi_L(m_2x)\psi'_L(m_1x) - m_1\,\psi'_L(m_2x)\psi_L(m_1x)}{m_2\chi_L(m_2x)\psi'_L(m_1x) - m_1\chi'_L(m_2x)\psi_L(m_1x)}, \tag{13}$$

$$B_L = \frac{m_2\psi_L(m_1x)\psi'_L(m_2x) - m_1\psi'_L(m_2x)\psi'_L(m_1x)}{m_2\chi'_L(m_2x)\psi_L(m_1x) - m_1\chi_L(m_2x)\psi'_L(m_1x)}, \tag{14}$$

where $m_1 = n_{\text{core}}/n_{\text{out}}$, $m_2 = n_{\text{shell}}/n_{\text{out}}$, $x = k_{\text{out}}r_{\text{core}}$ and $y = k_{\text{out}}r_{\text{shell}}$. $\psi_L(x) = xj_L(x)$, $\chi_L(x) = xN_L(x)$ and $\xi_L(x) = xh_L(y)$ are Riccati–Bessel, Riccati–Neumann and Riccati–Hankel functions, respectively. The prime ($'$) denotes derivation with respect to the argument.

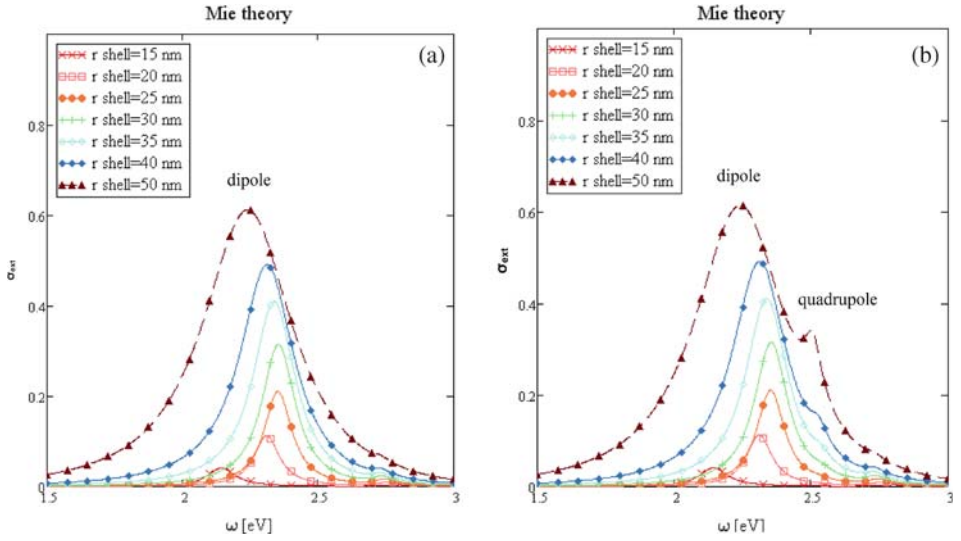

Figure 4. The extinction cross-section calculated based on the Mie theory for the nanoshell with a constant radius of the core and different radii of the shell, (**a**) for dipole mode SPR and (**b**) for both dipole and quadrupole SPR.

3. Result and discussion

The schematic representation of spherical metallic nanoshell, which is used for theoretical investigation in this work is depicted in figure 1 and the structural parameters used in modelling are presented in table 1. Figure 2a shows the calculated extinction cross-section as a function of energy for a spherical gold nanoshell with a different outer radius shell using both Mie theory and quasistatic method while the radius of the core is 10 nm and the refractive index of the core is 1.3. The figure shows two peaks representing the inner and outer surfaces. The splitting of the peak of the localized surface plasmon is explained by the existence of plasma fluctuations of electron density in particles not only on the outer surface of the particle but also on the inner surface of the metallic shell. When the radius of the shell increases, the surface plasmon resonance moves to higher energy. However, weak peaks shift to lower energy. The inset of figure 2a (Mie theory) shows the surface plasmon frequency as a function of the radius of the shell and the SPR energy depends on outer shell reduces and exponentially varies with increasing shell thickness.

The effect of core radius on SPR is shown in figure 2b while the outer radius of the shell is kept constant at 15 nm. The results show (figure 2b) that the surface plasmon peak (at the outer surface) shifts to lower energy due to the reduction of metal content in

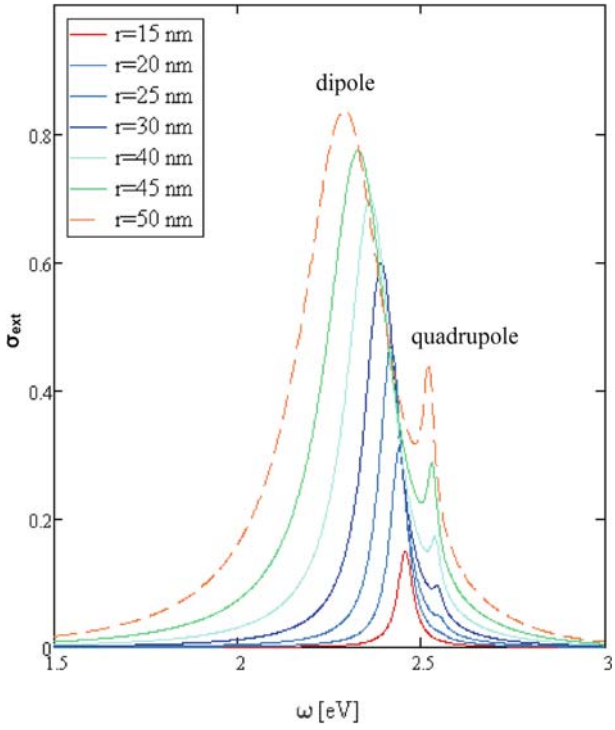

Figure 5. Extinction cross-section for gold nanospheres with radius ranging from 15 to 50 nm in a medium with $n_{\text{out}} = 1.5$.

the particle with increase in core radius. Therefore, the frequencies of both the surface plasmons depend on the thickness of the layers. Also, it should be noted that in both the cases, the content of metal fractions in particles of different species are different. As a result, the intensity and frequencies of these resonances depend on the entire set of internal parameters of the particle and increase with the increase in the outer radius or increase in the fraction of a metal part of the particle. In addition, the plasmon linewidth strongly depends on the shell thickness.

The effect of the environment and the core refractive indices [29] on the SPR energy is depicted in the inset of figures 3a, 3b (Mie theory). Thus, surface plasmon frequency can be more sensible to the change in refractive index in the core and the surroundings of the nanoshell. Also, SP frequency as a function of embedding medium and the core refractive index are shown in the inset of figures 3a and 3b, respectively. This result provides a broad applicability in the design and fabrication of new composite materials. With increasing imaginary part of the effective dielectric function, broadening of SPR and reduction in its intensity are observed simultaneously. These plots clearly show that by increasing refractive index of the surrounding environment of the nanoshell, the main peak displays a red shift while the small peaks remain unchanged. Therefore, the shift of this outer surface plasmon energy peak is suitable to probe the change in refractive index of the environment. In all the cases, quasistatic approximation is in accordance with the Mie theory, although the intensity and peak broadening are different.

When the size of nanoparticles is increased, the quasistatic approximation becomes invalid. So Mie theory was applied. Figure 4a depicts the extinction cross-section for the nanoshell with 10 nm core radius and the variable shell radius ranging from 15 to 50 nm. In this plot Mie theory was applied but only for $L = 1$ in a series of cross-section.

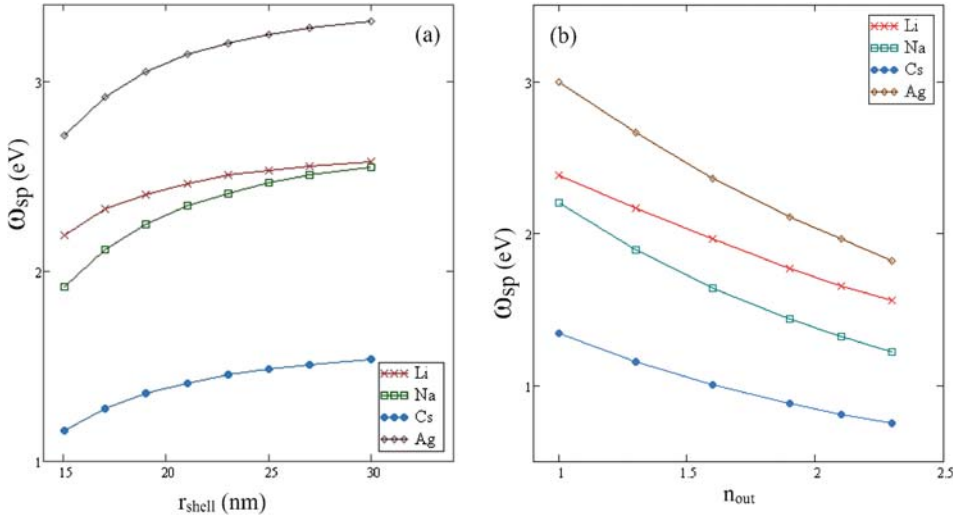

Figure 6. Surface plasmon energy as a function of (**a**) surrounding media having different refractive indices with $r_{\text{core}} = 10$ nm, $r_{\text{shell}} = 15$ nm, $n_{\text{core}}(SiO_2) = 1.5$ and (**b**) outer radius shell with $n_{\text{out}}(H_2O) = 1.3$, $r_{\text{core}} = 10$ nm, $n_{\text{core}}(SiO_2) = 1.5$. Calculations presented are from different metallic nanoshell materials.

It shows that from about $r_{\text{shell}} = 30\,\text{nm}$ the peak of the inner surface is pallid and the main peak shifts to lower energy. Extinction cross-section for gold nanosphere shown in figure 5 is similar to that depicted in figure 4b but with an accurate investigation about the contributions of higher-order multipolar (from $L = 1$ to 10) series of Mie theory cross-section which displays both dipole and quadrupole modes of SPR.

As shown in figure 6a, the SPR frequency is sensitive to variation of refractive index of the environment and can be tuned for higher energy with varied shell materials. Also, the calculated SPR frequency as a function of the outer shell radius for constant core radius is plotted in figure 6b. By increasing the thickness of the shell, the SPR frequency increases depending on the shell materials in different energy regions. Good agreement is seen between our calculated results and experimental reports [30–33].

4. Conclusions

The results obtained for spherical core–shell nanoparticles composed of a dielectric core and a metal shell with dimensions comparable to the wavelength of light calculated using the quasistatic approximation shows good agreement with the results obtained by Mie theory. For big nanostructures, the quasistatic approximation is invalid and Mie theory illustrates both the dipole and quadrupole SPRs in extinction cross-section. It was found that the SPR frequency shift was due to a change in refractive index of the environment of the metal nanoshell. Also, the SPR of metallic nanoshell displays size tuneability controlled by the ratio of the shell thickness to the core radius. The size dependency of the localized surface plasmon of metallic core–shell can be explained by assuming a size-dependent dielectric function. Furthermore, by increasing the metal content in particles the surface plasmon resonance peak at the outer surface of the metal shell tunes to higher energy. Thus, our results utilizing that by using the core–metal shell nanostructure with different types of core–shell material and size can tune the plasmonic resonance position in different spectral range depending to the practical involvement of the researchers.

Acknowledgements

The authors wish to acknowledge the University of Guilan for financial support.

References

[1] R D Averitt, S L Westcott and N J Halas, *J. Opt. Soc. Am. B* **16**, 1824 (1999)
[2] S Stolik, J A Delgado, A Pérez and L Anasagasti, *J. Photochem. Photobiol. B: Biol.* **57**, 90 (2000)
[3] V Ntziachristos, J Ripoll, L V Wang and R Weissleder, *Nature Biotechnol.* **23**, 313 (2005)
[4] W Y Chien and T Szkopek, *Opt. Express* **16**, 1820 (2008)
[5] S J Oldenburg, G D Hale, J B Jackson and N J Halas, *Appl. Phys. Lett.* **75**, 1063 (1999)
[6] J B Jackson, S L Westcott, L R Hirsch, J L West and N J Halas, *Appl. Phys. Lett.* **82**, 257 (2003)
[7] L Novotny and B Hecht, *Principles of nano-optics* (Cambridge University Press, Cambridge, 2006)

[8] M Quinten and U Kreibig, *Surf. Sci.* **172**, 557 (1986)
[9] C F Bohren and D R Huffman, *Absorption and scattering of light by small particles* (Wiley, New York, 1998)
[10] D R Link and M A El-Sayed, *Int. Rev. Phys. Chem.* **19**, 409 (2000)
[11] R D Averitt, D Sarkar and N Halas, *J. Phys. Rev. Lett.* **78**, 4217 (1997)
[12] S J Oldenburg, R D Averitt, S L Westcott and N J Halas, *Chem. Phys. Lett.* **288**, 43 (1998)
[13] S J Oldenburg, J B Jackson, S L Westcott and N J Halas, *Appl. Phys. Lett.* **75**, 2897 (1999)
[14] J L West, S R Sershen, N J Halas, S J Oldenburg and R D Averitt (In US Patent 6,428,811, USA, 2002)
[15] E Prodan and P Nordlander, *Nano Lett.* **3**, 543 (2003)
[16] E Prodan and P Nordlander, *J. Chem. Phys.* **120**, 5444 (2004)
[17] J Zhu and C L Zhang, *J. Appl. Phys.* **100**, 026104 (2006)
[18] S L Westcott, J B Jackson, C Radloff and N J Halas, *Phys. Rev. B* **66**, 155431 (2002)
[19] Xin Zhoua, Hongjian Li, Suxia Xie, Shaoli Fu, Haiqing Xu and Zhimin Liu, *Solid State Commun.* **151**, 1049 (2011)
[20] B T Draine and P J Flatau, *J. Opt. Soc. Am. A* **11**, 1491 (1994)
[21] A Pinchuk, U Kreibig and A Hilger, *Surf. Sci.* **557**, 269 (2004)
[22] U Kreibig, *J. Phys. F–Metal Phys.* **4**, 999 (1974)
[23] P Mulvaney, *Langmuir* **12**, 788 (1996)
[24] M Kerker, *Scattering of light and other electromagnetic radiation* (Academic, New York, 1969)
[25] G Mie, *Ann. Phys.* **25**, 377 (1908)
[26] U Kreibig and M Vollmer, *Optical properties of metal clusters* (Springer, Berlin, 1995)
[27] Michael Quinten, *Optical properties of nanoparticle systems: Mie and beyond* (Wiley-VCH Verlag & Co., KGaA, Germany, 2011)
[28] A L Aden and M Kerker, *J. Appl. Phys.* **22**, 1242 (1951)
[29] P B Johnson and R W Christy, *Phys. Rev. B* **6**, 4370 (1972)
[30] T Endo, D Ikeda, Y Kawakami, Y Yanagida and T Hatsuzawa, *Anal. Chem. Acta* **661**, 200 (2010)
[31] Jinmiao Zhu, Yuhua Shen, Anjian Xie and Lin Zhu, *J. Mater. Chem.* **19**, 8871 (2009)
[32] Q Fu, D G Zhang, M F Yi, X X Wang, Y K Chen, P Wang and H Ming, *J. Opt.* **14**, 085001 (2012)
[33] Q B Zhang, J P Xie, J Y Lee, J X Zhang and C Boothroyd, *Small* **4**, 1067 (2008)